Mechanistic Studies Examining the Efficiency and Fidelity of DNA Synthesis by the 3TC-Resistant Mutant (184V) of HIV-1 Reverse Transcriptase†

Joy Y. Feng and Karen S. Anderson*

Department of Pharmacology, Yale University School of Medicine, 333 Cedar Street, New Haven, Connecticut 06520-8066

Received March 26, 1999; Revised Manuscript Received May 24, 1999

ABSTRACT: A single amino acid substitution from methionine-184 to valine (M184V) of HIV-1 reverse transcriptase (RT) evokes the 1000-fold 3TC (Lamivudine) resistance by the HIV-1 virus observed in the clinic. The M184V mutant HIV-1 RT was studied to assess its catalytic efficiency during single nucleotide incorporation using a transient kinetic approach. The maximum rate of polymerization (k_{pol}), binding affinity (K_d), and incorporation efficiency (k_{pol}/K_d) were determined for incorporating dCTP and 3TC-TP by wild-type and 3TC-resistant HIV-1 RT. The 3TC-resistant HIV-1 RT showed a similar efficiency of incorporation compared with the wild-type enzyme during DNA-dependent DNA polymerization; however, the incorporation efficiency is reduced 3.5-fold during RNA-dependent polymerization. A dramatic 146- and 117-fold decrease in incorporation efficiency was observed for 3TC-MP incorporation by M184V RT for DNA- and RNA-dependent DNA polymerization, respectively, as compared with wild-type HIV-1 RT. While the k_{pol} was slower and the K_d was weaker for 3TC-TP incorporation by the M184V RT, the decrease in the efficiency of incorporation is primarily due to a substantially reduced binding affinity for the 3TC-TP to the enzyme•DNA (or RNA) complex poised for DNA elongation. The fidelity of M184V RT was also examined to evaluate mispair formation since this mutant has been suggested to exhibit a higher level of fidelity. The results of our studies indicate that there is a maximum 2.4-fold *increase* in fidelity for M184V RT as compared with wild-type HIV-1 RT. Both the wild-type and 3TC-resistant mutant RT showed higher fidelity using an RNA template as contrasted with the corresponding DNA template. This mechanistic information provides insight into our understanding of the molecular mechanism of 3TC-drug resistance and supports suggestions that increased RT fidelity and decreased fitness of the M184V HIV-1 virus may be factors contributing to the strong antiviral effect of AZT−3TC combination therapy.

Virally encoded human immunodeficiency virus type 1 (HIV-1) reverse transcriptase (RT)[1] is essential for viral replication and is the target of many clinically used drugs for treatment of acquired immunodeficiency syndrome (AIDS). Nucleoside analogues, such as AZT, ddC, ddI, and 3TC, serve as chain terminators after being phosphorylated to their active triphosphate form by cellular kinases and incorporated into DNA by HIV-1 RT. Though these analogues have showed high potency initially in the clinic, resistance to most of them develops rapidly due to the high frequency of viral mutation. Both in vitro and in vivo studies showed that the 3TC-resistant ($3TC^R$) HIV-1 virus has a 500−1000-fold reduced susceptibility caused by a single site mutation at codon 184 of the RT gene (*1*, *2*). The $3TC^R$ RT contains either an isoleucine (M184I) or a valine (M184V) at amino acid 184 instead of the methionine residue in the wild enzyme. In some cases, the M184I variant observed initially in patients was outgrown by the M184V variant, that was also reported in cell culture studies under high selective pressure (*1*, *2*). At a structural level, the Met-184 residue is located in the highly conserved YMDD motif, which contains two of the three conserved aspartic acid residues that comprise the RT polymerase active site (*3*−*5*). At a functional level, steady-state kinetic studies examining the polymerase activity have indicated that DNA- or RNA-dependent DNA synthesis of the M184V RT enzyme is 40−280% that of wild-type HIV-1 RT, depending upon the assay conditions employed (*6*−*12*). Moreover, virion-particle-derived $3TC^R$ HIV-1 RT exhibited a 28-fold decreased susceptibility toward 3TC compared with that of wild-type HIV-1 RT (*1*). Clinical studies have demonstrated that 3TC−AZT combination therapy results in a strong and sustained antiviral response, more than that anticipated from a simple additive inhibitory effect on HIV-1 RT (*13*, *14*). Cell culture studies suggested that the presence of the M184V variants might delay the generation of doubly resistant HIV-1 viruses in combination therapy (*8*, *15*). Several hypotheses

† This work was supported by NIH Grant GM49551 to K.S.A.

* To whom correspondence should be addressed: 333 Cedar St., New Haven, CT 06520-8066. Phone: 203-785-4526. E-mail: karen.anderson@yale.edu.

[1] Abbreviations: AIDS, acquired immunodeficiency syndrome; dATP, 2′-deoxyadenosine 5′-triphosphate; dGTP, 2′-deoxyguanosine 5′-triphosphate; dTTP, 2′-deoxythymidine 5′-triphosphate; dCMP, 2′-deoxycytidine 5′-monophosphate; dCTP, 2′-deoxycytidine 5′-triphosphate; dNTP, 2′-deoxynucleoside 5′-triphosphate; EDTA, (ethylenediamine)tetraacetate; HIV-1, human immunodeficiency virus type 1; RT, reverse transcriptase; (+)SddCTP, β-D-(+)-2′,3′-dideoxy-3′-thiacytidine; 3TC, 2′,3′-dideoxy-3′-thiacytidine; 3TC-MP, 2′,3′-dideoxy-3′-thiacytidine 5′-monophosphate; 3TC-TP or (−)SddCTP, β-L-(−)-2′,3′-dideoxy-3′-thiacytidine 5′-triphosphate; $3TC^R$, 3TC-resistant; Tris, tri(hydroxymethyl)aminomethane; WT, wild type.

10.1021/bi990709m CCC: $18.00
Published on Web 06/30/1999

have been proposed to explain the role of M184V residue substitution on in vivo virus evolution. These include enhanced replication fidelity of the M184V HIV-1 RT (*8*), decreased fitness of the mutant virus (*16*), and a requirement of more sites of mutation to reach coresistance to both 3TC and AZT (*9*). It is noteworthy that four or five amino acid substitutions (M41L, D67Q, K70R, T215Y, K219N) have been associated with AZT drug resistance (*17*−*20*).

Our laboratory (*21*−*24*) and others (*25*−*27*) have used a pre-steady-state kinetic analysis to establish the reaction pathway for HIV-1 RT. The reaction pathway is ordered in which the enzyme first binds to the DNA (or RNA) substrate to form a tight enzyme·DNA complex with a K_d value in the nanomolar range. The binding of the correct nucleoside triphosphate (dNTP) follows this step. After forming the initial enzyme·DNA·dNTP complex, the enzyme checks for the proper base-pairing geometry and then undergoes a slower conformational change, which limits chemical catalysis. The maximum rate of incorporation, k_{pol}, is governed by this conformational change. The last and also the slowest step in the overall reaction pathway involves the dissociation of the elongated DNA substrate from the enzyme. In contrast to a steady-state kinetic analysis which only reflects the slowest step in the overall reaction pathway, a transient kinetic approach allows one to examine each of the individual steps in the pathway including the identification of enzyme intermediates and conformational changes which might be associated with chemical catalysis.

A pre-steady-state kinetic analysis comparing the (−)3TC-TP interaction with wild-type and mutant forms of RT has been reported (*28*). This study indicated that there was little change in the relative K_d values for interaction of 3TC-TP with wild-type and mutant RT, although up to a 36-fold decrease in k_{pol} was noted (*28*). The K_d values for 3TC-TP measured in this study were suprisingly high (45−63 μM) considering the observed potency in other studies (*29*−*32*).

We have recently used a transient kinetic approach to examine the incorporation of natural and modified cytidine analogues {dCTP; ddCTP; β-D-(+)-2′,3′-dideoxy-3′-thiacytidine [(+)SddCTP]; and β-L-(−)-2′,3′-dideoxy-3′-thiacytidine [(−)SddCTP, (3TC-TP)]} in an effort to understand the mechanistic basis of inhibition of HIV-1 RT by 3TC-TP (*33*). The present study was designed to examine the effect of a single amino acid substitution at codon 184 (methionine to valine) on the incorporation of the natural substrate, dCTP, and the active triphosphate (3TC-TP) form of the 3TC[2] drug used clinically. We used a transient kinetic approach to determine the k_{pol}, K_d, and efficiency of incorporation (k_{pol}/K_d) for dCTP and 3TC-TP by the wild-type and M184V mutant HIV-1 RT. Furthermore, since the 3TC^R RT has been suggested to exhibit higher fidelity (*8, 11, 12, 34, 35*), we extended this analysis to examine misincorporation opposite a template deoxyguanosine and guanosine for DNA and RNA substrates during single nucleotide incorporation. Specific questions these studies were designed to address include the following: (1) Are there changes in the kinetic parameters for incorporating dCTP or 3TC-TP for wild type versus M184V mutant HIV-1 RT which may be linked to the molecular mechanism of drug resistance? (2) Are there differences in the incorporation efficiency during DNA-dependent, or RNA-dependent, DNA synthesis that may affect viral fitness? (3) Does the 3TC^R RT exhibit a higher fidelity for misincorporation as compared with wild type during DNA-dependent, or RNA-dependent, DNA polymerization? The results in this study provide a quantitative description of the interactions of dCTP and 3TC-TP with wild-type and 3TC^R RT during DNA-directed and RNA-directed DNA synthesis as well as mispair formation. The mechanistic information presented here provides a detailed kinetic and thermodynamic description of the wild-type and M184V RT reaction pathway and insight into understanding 3TC drug resistance at a molecular level.

MATERIALS AND METHODS

Overexpression and Purification of Wild-Type and 3TC-Resistant HIV-1 RT. HIV-1 RTs were purified as previously described (*21, 23*). The protein concentration of purified RT was measured spectrophotometrically at 280 nm using an extinction coefficient $\epsilon_{280} = 260\,450\ M^{-1}\ cm^{-1}$. The concentration of active RT was determined as previously described with pre-steady-state burst experiments that gave burst amplitudes in the range of 40−50%. The experiments described in the current study were performed using the corrected active site concentration.

Nucleotide Triphosphates and Other Materials. All dNTPs were purchased from Pharmacia LKB Biotechnology Inc. Dr. R. F. Schinazi (Emory University, Atlanta, GA) kindly provided the 3TC-TP. The purity of these compounds (>99%) was verified by HPLC analysis as well as LC/ESI mass spectrometry. [γ-^{32}P]ATP was purchased from Amersham. Biospin columns for the removal of excess nucleotide were purchased from Bio-Rad.

Synthetic Oligonucleotides. The DNA oligonucleotides (18- and 36-mer) shown in Table 1 were synthesized on an Applied Biosystems 380A DNA synthesizer (DNA synthesis facility, Yale University) and purified using denaturing polyacrylamide gel electrophoresis (16% acrylamide, 8 M urea). The RNA oligonucleotide (36-mer, Table 1) was synthesized and gel-purified by New England Biolabs.

The duplex 18/36-mer DNA/DNA and DNA/RNA primer-templates were formed by annealing an approximately 1:1.3 molar ratio of pure 18- and 36-mer at 80 °C for 4 min and 50 °C for 30 min. The duplex mixtures were analyzed by nondenaturing polyacrylamide gel electrophoresis (15%) to ensure that proper annealing had taken place. Concentrations of the oligonucleotides were estimated by UV absorbance at 260 nm using the following calculated extinction coefficients: DNA 18-mer, $\epsilon = 170\,000\ M^{-1}\ cm^{-1}$; DNA 36-mer, $\epsilon = 388\,000\ M^{-1}\ cm^{-1}$; RNA 36-mer, $\epsilon = 396\,000\ M^{-1}\ cm^{-1}$.

Buffers. All experiments using HIV-1 RT were carried out in 50 mM Tris-HCl, 50 mM NaCl buffer at pH 7.8 and at a temperature of 37 °C. All experimental procedures were carried out using sterile buffers, reagents, and glassware where feasible.

5′-^{32}P-Labeling of 18/36-mers. Before annealing, both primer and template strands of the DNA/RNA and DNA/

[2] The abbreviation 3TC is used to refer to the unnatural L or (−) isomer, (−)SddC. These are often used interchangeably. While we have used the common nomenclature in the literature, the most appropriate chemical nomenclature is (−)-*cis*-1-[2-(hydroxymethyl)-1,3-oxathiolan-5-yl]cytosine.

DNA 18/36-mer were 5′-radiolabeled with T4 polynucleotide kinase (New England Biolabs) according to previously described procedures (*21*).

Rapid Quench Experiments. Rapid chemical quench experiments were performed as previously described with a KinTek Instruments Model RQF-3 rapid-quench-flow apparatus (*21*, *23*). Unless noted otherwise, all concentrations refer to the final concentrations after mixing.

Pre-Steady-State Burst and Single-Turnover Experiments. A combination of pre-steady-state burst experiments and single-turnover experiments was used in this transient kinetic analysis. The pre-steady-state burst experiments were used to examine the incorporation of the next correct nucleotide into a DNA/DNA or DNA/RNA duplex at 37 °C during the first enzyme turnover as well as subsequent turnovers (*36*). This analysis was conducted under the conditions in which the duplex concentration was 3 times greater than the enzyme concentration. The reaction was carried out by mixing a solution containing the preincubated complex of 100 nM HIV-1 RT and 5′-labeled 300 nM DNA/RNA or DNA/DNA duplex with a solution of 10 mM Mg^{2+} and varying concentrations of dNTP (in the range of 0.5 μM to 7 mM). Polymerization was quenched with 0.3 M EDTA at time intervals ranging from 3 ms to 20 s. DNA polymerization products were quantified by sequencing gel analysis. The product formation occurred in a fast phase followed by a slow phase. The data were fitted to a burst equation (see *Data Analysis*). Single-turnover experiments which are conducted under conditions in which enzyme is in excess over radiolabeled oligonucleotide allow one to examine chemical catalysis during a single enzyme turnover (*36*). Due to the low rate of the incorporation for 3TC-TP, single-turnover experiments were used to determine the K_d and k_{pol} values for incorporation of 3TC-TP into a DNA/DNA or a DNA/RNA primer-template. Single-turnover experiments were performed in a manner similar to that described above except that enzyme (400 nM) was used in excess of 5′-labeled DNA/DNA or DNA/RNA duplex (100 nM). The misincorporation studies were all carried under single-turnover conditions (*37*). In the cases where long reaction times were required (as in the case for dATP and dGTP incorporation), manual quench experiments were undertaken in which the two solutions (primer-template preincubated with RT and dNTP−Mg^{2+}) were mixed and incubated at 37 °C, and at regular time intervals, 30 μL of the reaction solution was removed and quenched with EDTA.

Product Analysis. The products were analyzed by sequencing gel electrophoresis (20% acrylamide, 8 M urea, 1 × TBE running buffer), and the products were quantified using a Bio-Rad GS525 Molecular Imager (Bio-Rad Laboratories, Inc., Hercules, CA).

Data Analysis. Data were fitted by nonlinear regression using the program KaleidaGraph version 3.09 (Synergy Software, Reading, PA). Data from burst experiments were fitted to a burst equation: $[\text{product}] = A[1 - \exp(-k_{obsd}t) + k_{ss}t]$, where A represents the amplitude of the burst which correlates with the concentration of enzyme in active form, k_{obsd} is the observed first-order rate constant for dNTP incorporation, and k_{ss} is the observed steady-state rate constant. Data from single-turnover experiments were fit to a single exponential. The K_d, the dissociation constant of dNTP binding to the complex of RT and 18/36 DNA/DNA and DNA/RNA substrate, is calculated by fitting the data to the following hyperbolic equation: $k_{obsd} = k_{pol}[\text{dNTP}]/(K_d + [\text{dNTP}])$, where k_{pol} is the maximum rate of dNTP incorporation, [dNTP] is the corresponding concentration of dNTP, and K_d is the equilibrium dissociation constant for the interaction of dNTP with the E·DNA complex.

Table 1: Sequence of Oligonucleotide Substrates[a]

DNA/DNA 18/36-mer:

```
          5'-*G TCC CTG TTC GGG CGC CA-3'
3'-CGA AAG TCC AGG GAC AAG CCC GCG GTG ACG ATC TCT*-5'
```

DNA/RNA 18/36-mer:

```
          5'-*G TCC CTG TTC GGG CGC CA-3'
3'-CGA AAG UCC AGG GAC AAG CCC GCG GUG ACG AUC UCU*-5'
```

[a] An asterisk indicates 5′-^{32}P-labeling of the oligomer.

RESULTS

In this report, we compared the activities of wild-type with $3TC^R$ (M184V) RT in terms of correct incorporation of dCTP and 3TC-TP into a DNA/DNA or DNA/RNA primer-template, along with their activities in carrying out misincorporation. The 36-mer DNA or RNA template used in this study is identical to a region of the HIV-1 RNA genomic sequence, and the 18-mer DNA primer is complementary to the primer binding site (PBS). This 18/36-mer primer-template (Table 1) was chosen as a substrate for study due to its physiological relevance for HIV-1 viral replication and also to avoid problems which have previously been encountered with blunt-ended substrates (*38*, *39*). A series of pre-steady-state burst and single-turnover experiments were conducted to determine the kinetic parameters for correct incorporation of dCTP and 3TC-TP during DNA-directed, and RNA-directed, DNA synthesis by wild-type and $3TC^R$ RT. These kinetic parameters include the following: the maximum rate of incorporation, k_{pol}; the equilibrium dissociation constant, K_d; and the incorporation efficiency, k_{pol}/K_d. This information is important to provide a quantitative basis for understanding how alterations in the interactions of dCTP and 3TC-TP with the $3TC^R$ RT relative to wild-type RT confer drug resistance to 3TC.

These kinetic parameters were also measured for the incorporation of an incorrect dNTP (dTTP, dATP, and dGTP) opposite a DNA template (2′-deoxyguanosine) or an RNA template (guanosine), and the corresponding fidelity estimates were calculated as $[(k_{pol}/K_d)_{correct} + (k_{pol}/K_d)_{incorrect}]/(k_{pol}/K_d)_{incorrect}$. This information will allow a detailed assessment of whether there are changes in fidelity with $3TC^R$ RT relative to wild-type RT during DNA-dependent and/or RNA-dependent DNA polymerization.

Kinetics of Correct Incorporation

Incorporation of dCTP into DNA/DNA 18/36-mer Primer-Template by Wild-Type or $3TC^R$ HIV-1 RT. Our first step in defining the kinetic of correct incorporation was to conduct a pre-steady-state burst experiment with wild-type and $3TC^R$ RT. In this type of experiment, the DNA substrate is in excess of enzyme such that the first enzyme turnover as well as multiple turnovers can be examined. Our previous studies

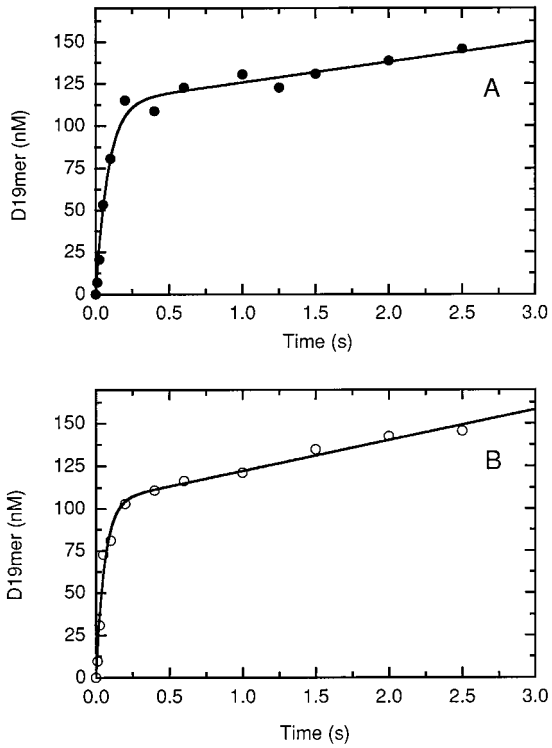

FIGURE 1: Pre-steady-state kinetics of incorporation of dCMP with wild-type (●) and 3TC^R (○) HIV-1 RT. (A) Pre-steady-state kinetics of incorporation of dCMP into a homoduplex DNA/DNA 18/36 primer-template by wild-type HIV-1 RT were measured by mixing a preincubated solution of wild-type RT (100 nM) and 18/36 DNA/DNA homoduplex (300 nM) with dCTP (10 μM) and Mg^{2+} (10 mM) under rapid quench conditions. The reactions were quenched at the indicated time and analyzed by sequencing gel electrophoresis. The solid line represents the best fit of the data (●) to a burst equation with an amplitude $A = 113 \pm 5$ nM, an observed first-order rate constant for the burst phase $k_{obsd} = 12 \pm 1$ s^{-1}, and an observed rate constant for the linear phase $k_{ss} = 0.11 \pm 0.03$ s^{-1} for the wild-type (●) HIV-1 RT. (B) Pre-steady-state kinetics of incorporation of dCMP into homoduplex DNA/DNA 18/36 primer-template as described in (A) using 3TC^R RT. The kinetic parameters are $A = 104 \pm 4$ nM, $k_{obsd} = 17 \pm 2$ s^{-1}, and $k_{ss} = 0.17 \pm 0.03$ s^{-1} for 3TC^R (○) HIV-1 RT.

with wild-type enzyme have shown a burst of product formation, an important diagnostic experiment indicating that product release limits the overall reaction pathway. To establish that the mechanistic pathway has not changed with 3TC^R RT, we compared the mutant enzyme with wild type in a pre-steady-state burst experiment as described under Materials and Methods. Representative time courses for the incorporation of dCMP (10 μM) into the homoduplex DNA/DNA 18/36-mer primer-template by wild-type (panel A) or 3TC^R RT (panel B) are shown in Figure 1.

A biphasic burst of product formation is observed in both cases. The solid lines represent the best fit of the data to a burst equation and give the following values: an amplitude $A = 113 \pm 5$ nM, an observed first-order rate constant for the burst phase $k_{obsd} = 12 \pm 1$ s^{-1}, and an observed rate constant for the linear phase $k_{ss} = 0.11 \pm 0.03$ s^{-1} for the wild type (●) and $A = 104 \pm 4$ nM, $k_{obsd} = 17 \pm 2$ s^{-1}, and $k_{ss} = 0.17 \pm 0.03$ s^{-1} for 3TC^R (○) HIV-1 RT. Clearly, the observation of a burst of product formation during single-nucleotide incorporation by mutant RT indicates that the mechanistic pathway has not changed.

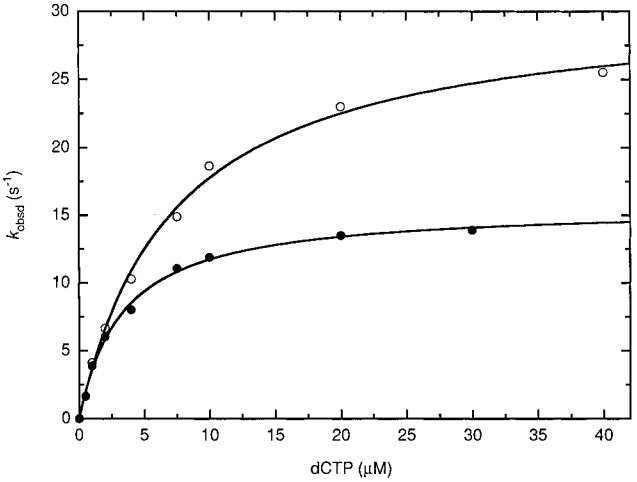

FIGURE 2: Concentration dependence of dCTP upon the observed rate, k_{obsd}, for dCMP incorporation into a DNA/DNA 18/36 primer-template by wild-type (●) or 3TC^R (○) HIV-1 RT. The first-order rates were plotted against dCTP concentration, and the data (●, ○) were fit to a hyperbola (solid line) to yield a K_d value of 3.4 ± 0.2 μM and a maximum rate of incorporation (k_{pol}) of 15.7 ± 0.3 s^{-1} for the wild-type (●) RT and a K_d of 7.0 ± 0.6 μM and k_{pol} of 30.5 ± 0.8 s^{-1} for the 3TC^R (○) HIV-1 RT, respectively.

A complete study of the dNTP concentration dependence on the observed burst rate of incorporation provides measurements for the dissociation constant K_d, the maximum rate of dNMP incorporation k_{pol}, and the efficiency of incorporation k_{pol}/K_d. Figure 2 shows the [dCTP] dependence on k_{obsd} for incorporation into the DNA/DNA 18/36-mer primer-template using wild-type (●) and mutant RT (○). The k_{pol} value for dCMP incorporation by 3TC^R RT (30.5 ± 0.8 s^{-1}) is 2-fold higher than that of the wild-type (15.7 ± 0.3 s^{-1}); however, the K_d value for the 3TC^R is also 2 times higher than wild-type RT, indicating a slightly weaker binding of dCTP to the E·DNA complex. A complete summary of k_{pol}, K_d, and k_{pol}/K_d values for each dNTP with wild-type or 3TC^R RT is shown in Table 2 for the DNA/DNA 18/36-mer primer-template substrate. The compensatory changes in the k_{pol} and K_d values result in very similar values for the incorporation efficiencies for wild-type and 3TC^R RT.

Incorporation of 3TC-TP into DNA/DNA 18/36-mer Primer-Template by Wild-Type or 3TC^R RT. Pre-steady-state burst experiments examining the incorporation of 3TC-TP into a DNA/DNA primer-template also revealed the biphasic burst of product formation for both wild-type and 3TC^R RT (data not shown) indicating a similar mechanism. The rate of incorporation of 3TC-TP, in each case, was rather slow relative to the natural substrate dCTP; therefore, single-turnover experiments were performed to determine the kinetic parameters as described under Materials and Methods. The 3TC-TP concentration dependence upon the observed rate (k_{obsd}) of incorporation of wild-type (●) and 3TC^R (○) HIV-1 RT provides the maximum rate of polymerization, k_{pol}, as shown in Figure 3. For the wild-type enzyme, the highest concentration of 3TC-TP chosen without observing an inhibitory effect was 1.25 μM. The K_d curve for the wild-type RT was replotted to scale and is shown in the inset. As seen in our earlier studies, 3TC-TP is incorporated more slowly than the dCTP, but binds more tightly to the E·DNA complex than the natural substrate (*33*). The 3TC^R RT incorporates 3TC-TP with a k_{pol} value 2-fold slower than

Table 2: Kinetic Differences between Wild-Type and 3TC^R HIV-1 RT in DNA- or RNA-Dependent Incorporation of dCTP or 3TC-TP

primer/template	nucleotide	RT	k_{pol} (s^{-1})	K_d (μM)	k_{pol}/K_d (μM^{-1} s^{-1})[a]	selectivity factor[b]
DNA/DNA	dCTP	WT	15.7 ± 0.3	3.4 ± 0.2	4.6 ± 0.3	13
	3TC-TP	WT	0.046 ± 0.002	0.13 ± 0.02	0.35 ± 0.06	
	dCTP	3TC^R	30.5 ± 0.8	7.0 ± 0.6	4.4 ± 0.4	1830
	3TC-TP	3TC^R	0.024 ± 0.003	10 ± 3	(2.4 ± 0.7) × 10^{-3}	
DNA/RNA	dCTP	WT	37 ± 1	8.7 ± 0.9	4.2 ± 0.4	20
	3TC-TP	WT	0.051 ± 0.003	0.24 ± 0.03	0.21 ± 0.03	
	dCTP	3TC^R	63 ± 4	52 ± 8	1.2 ± 0.2	670
	3TC-TP	3TC^R	(9.2 ± 0.6) × 10^{-3}	5.2 ± 0.9	(1.8 ± 0.3) × 10^{-3}	

[a] Errors in the values of k_{pol}/K_d were calculated using standard methods (*53*). [b] Defined as $(k_{pol}/K_d)_{dCTP}/(k_{pol}/K_d)_{3TC-TP}$.

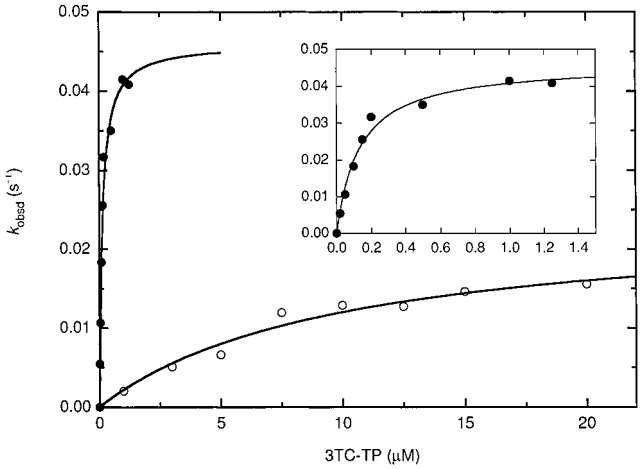

FIGURE 3: Concentration dependence of 3TC-TP upon the observed rate, k_{obsd}, for 3TC-MP incorporation into a DNA/DNA 18/36 primer-template by wild-type (●) or 3TC^R (○) HIV-1 RT on the concentration of 3TC-TP. The first-order rates were plotted against 3TC-TP concentration, and the data (●, ○) were fit to a hyperbola (solid line) to yield a K_d value of 0.13 ± 0.02 μM and a maximum rate of incorporation (k_{pol}) of 0.046 ± 0.002 s^{-1} wild-type (●) RT and a K_d of 10 ± 3 μM and k_{pol} of 0.024 ± 0.003 s^{-1} for the 3TC^R (○) HIV-1 RT, respectively. Inset: The data for wild-type (●) HIV-1 RT were replotted to scale to provide a better view of the curve fit.

the wild-type RT, and, more interestingly, this mutant has a 77-fold weaker K_d for the affinity of 3TC-TP (10 μM versus 0.13 μM). The combined effects on k_{pol} and K_d lead to a dramatic 146-fold difference in the efficiency of incorporation, k_{pol}/K_d, between the wild-type and 3TC^R RT (0.35 μM^{-1} s^{-1} versus 2.4 × 10^{-3} μM^{-1} s^{-1}) (see Table 2).

Correct Incorporation of dCTP into DNA/RNA 18/36-mer Primer-Template by Wild-Type or 3TC^R RT. Pre-steady-state burst experiments were performed under conditions described under Materials and Methods. A biphasic burst of product formation was observed in both RT enzymes (data not shown), indicating that the kinetics of RNA-dependent DNA polymerization by mutant RT are mechanistically similar to those of the wild-type RT. A complete study of the dCTP concentration dependence on the observed burst rate of incorporation was conducted, and the kinetic parameters are shown in Table 2. The high rate of dCMP incorporation by 3TC^R RT (63 ± 4 s^{-1}) versus that of the wild type (37 ± 1 s^{-1}) is compensated by the fact that the K_d value for 3TC^R (52 ± 8 μM) is much higher than that of wild-type RT (8.7 ± 0.9 μM). This translates into a 3−4-fold higher efficiency of incorporation (k_{pol}/K_d) for wild-type RT as compared with 3TC^R RT during RNA-dependent DNA synthesis.

Correct Incorporation of 3TC-TP into DNA/RNA 18/36-mer Primer-Template by Wild-Type or 3TC^R RT. Similar to the results described above, pre-steady-state burst experiments showed that there was no change in mechanism between wild-type and mutant enzyme in incorporating 3TC-TP into a DNA/RNA substrate (data not shown). Single-turnover experiments were performed under conditions described under Materials and Methods. Similar to what we have observed in the DNA-dependent DNA polymerization, 3TC-TP has a slower k_{pol} but a tighter affinity to the E·RNA complex than dCTP. The mutant enzyme incorporates 3TC-TP almost 120 times less efficiently than the wild-type RT, due to a 6-fold slower k_{pol} and a 22-fold weaker binding affinity (K_d) for 3TC-TP.

Kinetics of Misincorporation

Misincorporation of dNTP into DNA/DNA 18/36-mer Primer-Template by Wild-Type or 3TC^R RT. The kinetics of misincorporation of the three deoxynucleoside triphosphates, dTTP, dATP, and dGTP, into the homoduplex DNA/DNA 18/36-mer were determined. The experiments with dTTP using either wild-type or 3TC^R RT were performed using a rapid chemical quench apparatus while those for dATP and dGTP were conducted using manual quenching methods (*37*). Single-turnover experiments were performed to measure the k_{obsd} under selected concentrations of the dNTPs. Substrate inhibition occurred with dNTP concentrations in excess of 3−7 mM as previously observed (*21*, *37*). All products formed were quantitated. The kinetic parameters for incorrect incorporation into the homoduplex DNA/DNA 18/36-mer primer-template are summarized in Table 3. The DNA-dependent DNA replication fidelity was estimated from the ratios of incorporation of the second-order rate constants for correct to incorrect, as calculated by the expression shown in Table 3.

For the 3TC^R RT, the fidelity estimates for the dG·dT, dG·dA, and dG·dG mismatches were 4000, 86 000, and 150 000, respectively. In contrast, the fidelity estimates for the wild-type RT for misincorporation involving the dG·dT, dG·dA, and dG·dG mismatches were 1700, 77 000, and 85 000, respectively, for the wild-type RT. Thus, there is clearly a >2-fold *increase* in fidelity for the 3TC^R RT compared with wild type in forming a purine-pyrimidine dG·dT mismatched base pair. Less substantial differences between wild-type and mutant enzymes were noted with the purine-purine mismatches.

Misincorporation of dNTP into DNA/RNA 18/36-mer Primer-Template by Wild-Type or 3TC^R RT. The kinetics of misincorporation of the three incorrect deoxynucleoside triphosphates, dTTP, dATP, and dGTP, into the heteroduplex DNA/RNA 18/36-mer opposite a template guanosine were also examined. The experiments were performed in a manner

Table 3: Misincorporation by Wild-Type and 3TC^R HIV-1 RT into D18/D36 Primer-Template

nucleotide	RT	K_{pol} (s^{-1})	K_d (μM)	k_{pol}/K_d (μM^{-1} s^{-1})[a]	fidelity[b]
dCTP	WT	15.7 ± 0.3	3.4 ± 0.2	4.6 ± 0.3	
	3TC^R	30.5 ± 0.8	7.0 ± 0.6	4.4 ± 0.4	
dTTP	WT	1.11 ± 0.06	410 ± 60	$(2.7 \pm 0.4) \times 10^{-3}$	1700
	3TC^R	1.00 ± 0.04	890 ± 100	$(1.1 \pm 0.1) \times 10^{-3}$	4000
dATP	WT	0.12 ± 0.01	2000 ± 300	$(6.0 \pm 0.9) \times 10^{-5}$	77000
	3TC^R	0.066 ± 0.005	1300 ± 200	$(5.1 \pm 0.9) \times 10^{-5}$	86000
dGTP	WT	$(5.9 \pm 0.2) \times 10^{-3}$	110 ± 10	$(5.4 \pm 0.5) \times 10^{-5}$	85000
	3TC^R	$(6.4 \pm 0.2) \times 10^{-3}$	220 ± 20	$(2.9 \pm 0.3) \times 10^{-5}$	150000

[a] Errors in the values of k_{pol}/K_d were calculated using standard methods (*53*). [b] Calculated as $[(k_{pol}/K_d)_{correct} + (k_{pol}/K_d)_{incorrect}/(k_{pol}/K_d)_{incorrect}$.

Table 4: Misincorporation by Wild-Type and 3TC^R HIV-1 RT into D18/R36 Primer-Template

nucleotide	RT	K_{pol} (s^{-1})	K_d (μM)	k_{pol}/K_d (μM^{-1} s^{-1})[a]	fidelity[b]
dCTP	WT	37 ± 1	8.7 ± 0.9	4.2 ± 0.4	
	3TC^R	63 ± 4	52 ± 8	1.2 ± 0.2	
dTTP	WT	2.6 ± 0.1	1900 ± 200	$(1.3 \pm 0.1) \times 10^{-3}$	3200
	3TC^R	0.90 ± 0.07	4200 ± 700	$(2.1 \pm 0.4) \times 10^{-4}$	5700
dATP	WT	0.028 ± 0.001	2500 ± 100	$(1.1 \pm 0.1) \times 10^{-5}$	380000
	3TC^R	0.04 ± 0.01	10000 ± 5000	$(4 \pm 2) \times 10^{-6}$	300000
dGTP	WT	$(4.5 \pm 0.1) \times 10^{-3}$	280 ± 20	$(1.6 \pm 0.1) \times 10^{-5}$	260000
	3TC^R	$(4.4 \pm 0.2) \times 10^{-3}$	650 ± 80	$(6.8 \pm 0.9) \times 10^{-6}$	180000

[a] Errors in the values of k_{pol}/K_d were calculated using standard methods (*53*). [b] Calculated as $[(k_{pol}/K_d)_{correct} + (k_{pol}K_d)_{incorrect}]/(k_{pol}/K_D)_{incorrect}$.

similar to those studies described above which evaluated the use of a DNA/DNA 18/36-mer primer-template. Substrate inhibition occurred with dNTP concentrations in excess of 3−7 mM as previously observed (*21, 37*). In the case of dATP incorporation by 3TC^R RT, it became difficult to get an accurate measurement because the substrate inhibition occurred at a concentration lower than the prospective K_d. The kinetic parameters for incorrect incorporation into the heteroduplex DNA/RNA 18/36-mer primer-template are summarized in Table 4. For the 3TC^R RT, the fidelity estimates for the rG•dT, rG•dA, and rG•dG mismatches were 5700, 300 000, and 180 000, respectively, in comparison to 3200, 380 000, and 260 000 for the wild-type RT.

The weaker binding affinity of dTTP to the 3TC^R RT and its slower incorporation rate lead to a 6-fold lower (misincorporation) efficiency for the mutant RT compared with the wild-type RT, however, the fidelity increase for the 3TC^R RT is only 1.8-fold because of its lower $(k_{pol}/K_d)_{correct}$, efficiency in correct incorporation.

DISCUSSION

In this paper, we have examined the kinetics for the correct incorporation of dCMP and 3TC-MP and the incorrect incorporation of dTMP, dAMP, and dGMP into a DNA/DNA and DNA/RNA primer-template catalyzed by both wild-type and 3TC-resistant (M184V) HIV-1 RT. Our studies have focused on identifying altered kinetic parameters for incorporating dCTP or 3TC-TP for wild-type versus 3TC^R mutant HIV-1 RT in an effort to understand the molecular basis for the M184V amino acid substitution that confers drug resistance to 3TC. A related goal was to distinguish features of the reaction kinetics such as changes in the incorporation efficiency during DNA-dependent, or RNA-dependent, DNA synthesis that may be underlying factors in impacting the viral fitness for wild-type versus 3TC^R virus. An additional focus was to use a detailed transient kinetic analysis to discern whether the 3TC^R RT exhibits a higher fidelity for misincorporation as compared with wild-type enzyme, and, if so, which mispairs are involved.

Mechanistic Basis of 3TC Drug Resistance. Our studies have shown dramatic differences in the kinetic parameters for incorporating 3TC-TP by 3TC^R RT as compared with wild-type enzyme. The incorporation efficiencies for 3TC^R RT are 117- and 146-fold lower during RNA-dependent and DNA-dependent DNA synthesis, respectively. While the maximum rate of polymerization is lower and the affinity is weaker, the decreased incorporation efficiency primarily reflects a substantial change in the K_d value. The ratio of efficiency values for incorporation of the natural substrate, dCTP, versus the nucleoside analogue, 3TC-TP, defines the *selectivity* of RT. A comparison of the selectivities for wild-type (a factor of 13) and 3TC^R RT (a factor of 1830) reveals that the mutant enzyme now has a 141-fold higher selectivity for dCTP over 3TC-TP during DNA-directed DNA synthesis (Table 2). Similar results are observed for RNA-directed DNA synthesis. These altered kinetic parameters for the 3TC^R RT are most likely responsible the 1000-fold resistance of 3TC observed in vivo and in cell culture (*1, 2, 40*−*42*).

The structural basis of the drug resistance and altered kinetic parameters for the M184V mutation has not yet been resolved. The methionine 184 is part of the YXDD region that is highly conserved among reverse transcriptases, and most retroviral RTs have a methionine residue as amino acid X (*43, 44*). While functional studies have shown that the two Asp residues are a part of the catalytic triad and directly involved in the chemical catalysis, the function of Tyr-183 and Met-184 in HIV-1 RT is not clearly understood. A recent study showed that loss of polymerase activity due to a Y183F (Tyr to Phe) substitution could be compensated by a second M184V mutation (*45*). The recently solved three-dimensional structure of the DNA•(HIV-1 RT)•dNTP complex shows that M184V is located in the hairpin turn that connects β-sheets 9 and 10 (*5*). The methionine side chain contacts the base and the sugar moiety of the 3′-nucleotide in the primer, as would be expected for the β-branched side chain of a valine substitution as well. When a 3TC-TP was modeled into the structure, a greater interference was expected compared to a natural dNTP (*5*). If 3TC-TP binds in a conformation

similar to the natural substrate, dCTP, it must adopt an appropriate conformation to maintain proper base pairing. Since 3TC-TP has the unnatural (−)-L-configuration, the ribose ring must be positioned in the opposite orientation, with the CH_2 and 3′-S pointing toward the 3′ end of the primer and the O atom pointing in the opposite direction, causing increased distortion and/or steric hindrance (*33*). Due to the close proximity of the M184 residue to the polymerase active site, it has been speculated that the methionine may have multiple interactions with the primer-template, dNTP, and the surrounding amino acid residues comprising the dNTP binding pocket (*45*).

Thus, the structural consequences of the M184V mutation could render the incorporation of 3TC-TP unfavorable, as reflected in the substantially weakened affinity for the E·DNA complex discerned in our mechanistic studies.

Efficiency of Incorporation. The efficiency of nucleotide incorporation (k_{pol}/K_d) reflects the catalytic efficiency to carry out DNA-directed or RNA-directed DNA polymerization. The in vitro activity of the M184V mutant enzyme has been studied in many different assay systems to determine whether the incorporation efficiency is higher or lower relative to wild-type enzyme. In most cases, this usually involved assessing the polymerase activity under steady-state conditions by quantifying the amount of product formed with a fixed concentration of substrates, and the activity of mutant RT was reported as a percentage relative to the wild-type RT. This type of approach has been inconclusive since the activity of M184V RT has been reported in the range of 40−280% in different systems (*6, 7, 9, 10, 45*), suggesting that the efficiency is lower in some cases and higher in others. For instance, using homopolymeric primer-templates, a steady-state kinetic analysis revealed that the efficiency of the polymerization reaction (k_{cat}/K_m) for M184V RT varied from 0.75- to 3.2-fold that for the wild-type RT using an RNA template and 2−3-fold using a DNA template (*11*). The major disadvantage with a steady-state kinetic analysis, especially in addressing mechanistic issues related to polymerases, is that k_{cat} values reflect the slowest step in the overall pathway and K_m is a complex parameter, which may or may not be equal to the K_d value.

Our studies have focused on using a transient kinetic approach to directly measure the maximum rate of polymerization, k_{pol}, and binding affinity, K_d, for dCTP and 3TC-TP using physiologically relevant DNA and RNA substrates which contain HIV-1 genomic sequences. The ratio k_{pol}/K_d thereby defines the incorporation efficiency. As we have seen in other studies where completely different sequences were used, the incorporation of the natural substrate dCTP is much faster than the analogue 3TC-TP (*33*). However, 3TC-TP exhibited a higher affinity (lower K_d) toward the complex E·DNA (or E·RNA) than dCTP. For both dCTP and 3TC-TP, a higher k_{pol} is almost always observed in RNA-dependent DNA polymerization than in a DNA-dependent one, as reported in earlier studies (*21, 23, 33, 37*). In our study, we found that for both DNA- and RNA-dependent dCMP incorporation, $3TC^R$ RT showed a nearly 2-fold increase in k_{pol}. However, this does not directly translate into a higher efficiency of incorporation for $3TC^R$, as it was significantly compromised by the reduced affinity of dCTP for the mutant RT. Overall, the efficiency of DNA-dependent DNA polymerization by $3TC^R$ RT is similar to the wild-type RT, but is 3.5-fold lower than the wild-type enzyme in RNA-dependent incorporation. While we cannot rule out differences in sequence specificity between wild-type and mutant RT, very similar results were obtained when an entirely different sequence was used. In that study, the incorporation of dCTP into a random sequence D23/D45 primer-template (*33*) by mutant RT was as efficient as the wild-type enzyme; however, for the RNA-dependent incorporation, mutant RT is 3.7-fold less efficient than the wild-type RT (data not shown). Although the actual values for incorporation efficiency may be sequence-dependent, the general trend of lower incorporation efficiency for mutant RT during RNA-dependent DNA synthesis was observed in both of the sequences we tested.

Mutational studies have shown that there is a direct correlation between RT polymerase activity (hence incorporation efficiency) and the virus replication level (*46*). The level of viral replication is often expressed in terms of virus infectivity in which the level of virus antigen capsid protein p24 (CA-p24) is monitored during cell culture. A comparison of wild-type HIV-1 with the $3TC^R$ virus using this approach has shown that the levels of infectivity are similar, although a delay in replication was observed for the mutant virus (*9*). Another indicator to assess the replication ability of wild-type versus mutant virus involves measuring viral fitness. In this approach, the fitness of the mutant virus is measured by growth competition assays, in which a mixture of wild-type and mutant virus would result in the eventual selection of the fittest virus. The virus containing the M184V mutation has been show by this type of assay to have a lower level of fitness relative to wild type (*9, 14*). Moreover, DNA sequencing studies have shown that the high level of resistance to 3TC in vivo is due to the Met to Val substitution at codon 184 of the HIV-1 RT gene (*40*−*42*). It is likely that the decreased level of viral fitness for the M184V virus is linked to the decreased polymerase activity and a correspondingly lower incorporation efficiency in the 184V RT (*9*). Thus, our in vitro, detailed mechanistic studies on the M184V RT suggest that a reduced incorporation efficiency during RNA-directed DNA synthesis may contribute to the lower viral fitness observed in cell culture.

Fidelity of DNA Synthesis. HIV-1 RT is a highly error-prone reverse transcriptase due to a lack of 3′-5′-proofreading exonuclease activity. Although there are host cellular polymerases involved in HIV-1 virus replication, HIV-1 RT is generally believed to be the major cause of high mutation rate in HIV (*47, 48*). This genetic variation of HIV-1 virus hinders the host immunological response and the long-term efficacy of anti-HIV therapy (*48*). HIV-1 RT can make a number of errors, including misincorporation, mispair-extensions, and slippage-mediated frameshift errors (*49*). Also, the effect of a mutation on one of these different error types does not necessarily have a synergistic effect on the others, and in some cases, it may even be counterbalanced by the effects on another error type (*50*).

Several studies have shown that the M184V variant of HIV-1 RT has a higher fidelity than that of the wild-type RT. Using a DNA template, M184V RT showed higher fidelity in several mispair formation studies, and was reported as 2−17-fold (*8*), 6-fold (*34*), and 25−45-fold (*11*) increases compared with the wild-type enzyme. A 3−49-fold decreased error frequency was also reported for M184V RT in mispair-

extension assays using an RNA template (*12*). Read-through assays designed to reflect both misincorporation and mispair-extension efficiencies suggested that M184V RT had a lower read-through efficiency, which could suggest a higher fidelity for M184V RT. However, the interpretation of this result was complicated by a decreased processivity of M184V RT (*34*). In an effort to address the overall fidelity of M184V RT, an M13-based gap-filling assay was performed and a 1.6-fold decrease in the overall error rate was reported for M184V RT (*35*).

In the present study, we have directly examined the misincorporation of dNTP against a 2′-deoxyguanosine in a DNA template or a guanosine in an RNA template by directly measuring k_{pol}, K_d, and k_{pol}/K_d relative to correct incorporation. A small (2.4-fold) increase in the fidelity of M184V was observed. In general agreement with earlier studies from our laboratory, the RNA-dependent DNA polymerization has a higher fidelity than the DNA-dependent one in mispair formation (*37*). Also, similar to the steady-state results, the chance for a purine-pyrimidine mispair is at least 1−2 orders of magnitude higher than that for a purine-purine mispair.

Mechanistic Considerations for AZT−3TC Combination Therapy. Clinical studies have shown a synergistic effect when a combination of 3TC−AZT therapy is used to treat AIDS patients. The mechanistic basis of the success of combination therapy is not entirely clear. A number of studies have addressed the AZT−3TC synergistic effect at an in vivo level and in cell culture (*8*, *15*, *40*, *51*, *52*).

For instance, cell culture studies showed that the presence of the M184V mutation delays the development of coresistance to other nucleoside or nonnucleoside RT inhibitors, and introduction of a Val substitution at codon 184 into a background of AZT resistance RT gene suppressed the effect of AZT-resistance (*8*, *15*, *51*). An in vivo study demonstrated that multiple substitutions are required for the virus M184V harboring the mutation to reach the same level of AZT resistance; in contrast, one substitution is sufficient for observation of resistance in AZT monotherapy (*52*). It has been proposed that these factors, including the increased fidelity and the decreased fitness of M184V virus, as well as the suppressive effect of the M184V mutation on the development of a secondary drug resistance, can all contribute to the strong and sustained antiviral response with the combination of AZT and 3TC.

Summary. The present study has demonstrated that the 3TC-resistant (M184V) HIV-1 RT has a significantly lower efficiency in incorporating 3TC-MP compared with the wild-type RT, showing a clear correlation with the high level of resistance of M184V virus to 3TC reported in cell culture and in vivo. Moreover, a substantial decrease in incorporation efficiency was noted for the M184V mutant enzyme during RNA-directed DNA synthesis, providing a clear indication of at least one of the factors that may contribute to a decreased fitness for the mutant virus. This study has also revealed a small but significant increase in the fidelity of M184V in terms of mispair formation. We always exercise caution in explaining events occurring in vivo based upon in vitro experiments as well as drawing general conclusions about the properties of wild and mutant HIV-1 RT based upon a limited number of primer-template substrates which may be subject to local sequence effects. With these caveats in mind, the mechanistic information presented here provides a basis for interpreting 3TC drug resistance at a molecular level and provides insight into underlying mechanistic factors in the M184V HIV-1 RT that may contribute to a more detailed understanding of AZT−3TC combination therapy.

ACKNOWLEDGMENT

We thank Dr. Raymond Schinazi for the generous gift of 3TC-TP and Dr. Stephen Hughes, Dr. Paul Boyer, and Dr. Andrea Ferris for the HIV-1 RT wild-type and M184V mutant clones.

REFERENCES

1. Schinazi, R. F., Lloyd, R. M., Jr., Nguyen, M. H., Cannon, D. L., McMillan, A., Ilksoy, N., Chu, C. K., Liotta, D. C., Bazmi, H. Z., and Mellors, J. W. (1993) *Antimicrob. Agents Chemother. 37*, 875−881.
2. Schuurman, R., Nijhuis, M., van Leeuwen, R., Schipper, P., Collis, P., Danner, S. A., Mulder, J., Loveday, C., Christopherson, C., Kwok, S., Sninsky, J., and Boucher, C. A. B. (1995) *J. Infect. Dis. 171*, 1411−1419.
3. Kohlstaedt, L. A., Wang, J., Friedman, J. M., Rice, P. A., and Steitz, T. A. (1992) *Science 256*, 1783−1790.
4. Jacobo-Molina, A., Ding, J., Nanni, R. G., Clark, A. D., Lu, X., Tantillo, C., Williams, R. L., Kamer, G., Ferris, A. L., Clark, P., Hizi, A., Hughes, S. H., and Arnold, E. (1993) *Proc. Natl. Acad. Sci. U.S.A. 90*, 6320−6324.
5. Huang, H., Verdine, G. L., Chopra, R., and Harrison, S. C. (1998) *Science 282*, 1669−1675.
6. Wakefield, J. K., Jablonski, S. A., and Morrow, C. D. (1992) *J. Virol. 66*, 6802−6812.
7. Boyer, P. L., and Hughes, S. (1995) *Antimicrob. Agents Chemother. 39*, 1624−1628.
8. Wainberg, M. A., Drosopoulos, W. C., Salomon, H., Hsu, M., Borkow, G., Parniak, M. A., Gu, Z., Song, Q., Manne, J., Islam, S., Castriota, G., and Prasad, V. R. (1996) *Science 271*, 1282−1285.
9. Back, N. K. T., Nijhui, M., Keulen, W., Boucher, C. A. B., Oude Essink, B. B., van Kuilenburg, A. B. P., van Gennip, A. H., and Berkhout, B. (1996) *EMBO J. 15*, 4040−4049.
10. Chao, S.-F., Chan, V.-L., Juranka, P., Kaplan, A. H., Swanstrom, R., and Hutchison, C. A. I. (1995) *Nucleic Acids Res. 23*, 803−810.
11. Pandey, V., Kaushik, N., Rege, N., Sarafianos, S. G., Yadav, P. N. S., and Modak, M. J. (1996) *Biochemistry 35*, 2168−2179.
12. Hsu, M., Inouye, P., Rezende, L., Richard, N., Li, Z., Prasad, V. R., and Wainberg, M. A. (1997) *Nucleic Acids Res. 25*, 4532−4536.
13. Eron, J. J., Benoit, S. L., Jemsek, J., MacArthur, R. D., Santana, J., Quinn, J. B., Kuritzkes, D. R., Fallon, M. A., and Rubin, M. (1995) *N. Engl. J. Med. 333*, 1662−1669.
14. Larder, B. A., Kemp, S. D., and Harrigan, P. R. (1995) *Science 269*, 696−699.
15. Wainberg, M. A. (1997) *Leukemia 11 (Suppl. 3)*, 85−88.
16. Preston, B. D. (1997) *Science 275*, 228−229.
17. Larder, B. A., and Kemp, S. D. (1989) *Science 246*, 1155−1158.
18. Larder, B. A., Kellam, P., and Kemp, S. D. (1991) *AIDS 5*, 137−144.
19. Larder, B. A. (1994) *J. Gen. Virol. 75*, 951−957.
20. Kellam, P., Boucher, C. A., and Larder, B. A. (1992) *Proc. Natl. Acad. Sci. U.S.A. 89*, 1934−1938.
21. Kati, W. M., Johnson, K. A., Jerva, L. F., and Anderson, K. S. (1992) *J. Biol. Chem. 267*, 25988−25997.
22. Spence, R. A., Anderson, K. S., and Johnson, K. A. (1995) *Science 267*, 988−993.
23. Kerr, S. G., and Anderson, K. S. (1997) *Biochemistry 36*, 14064−14070.
24. Vaccaro, J. A., and Anderson, K. S. (1998) *Biochemistry 37*, 14189−14194.

25. Hsieh, J. C., Zinnen, S., and Modrich, P. (1993) *J. Biol. Chem. 268*, 24607−24613.
26. Reardon, J. E. (1993) *J. Biol. Chem. 268*, 8743−8751.
27. Rittinger, K., Divita, G., and Goody, R. S. (1995) *Proc. Natl. Acad. Sci. U.S.A. 92*, 8046−8049.
28. Krebs, R., Immendörfer, U., Thrall, S. H., Wöhrl, B. M., and Goody, R. S. (1997) *Biochemistry 36*, 10292−10300.
29. Faraj, A., Agrofoglio, L. A., Wakefield, J. K., McPherson, S., Morrow, C. D., Gosselin, G., Mathe, C., Imbach, J.-L., Schinazi, R. F., and Sommadossi, J.-P. (1994) *Antimicrob. Agents Chemother. 38*, 2300−2305.
30. Cherrington, J. M., Fuller, M. D., Mulato, A. S., Allen, S. J. W., Kunder, S. C., Ussery, M. A., Lesnikowski, Z., Schinazi, R. F., Sommadossi, J.-P., and Chen, M. S. (1996) *Antimicrob. Agents Chemother. 40*, 1270−1273.
31. Gray, N. M., Marr, C. L., Penn, C. R., Cameron, J. M., and Bethell, R. C. (1995) *Biochem. Pharmacol. 50*, 1043−1051.
32. Ueno, T., and Mitsuya, H. (1997) *Biochemistry 36*, 1092−1099.
33. Feng, J. Y., and Anderson, K. S. (1999) *Biochemistry 38*, 55−63.
34. Oude Essink, B. B., Back, N. K., and Berkhout, B. (1997) *Nucleic Acids Res. 25*, 3212−3217.
35. Rezende, L. F., Drosopoulos, W. C., and Prasad, V. R. (1998) *Nucleic Acids Res. 26*, 3066−3072.
36. Johnson, K. A. (1992) *Enzymes (3rd Ed.) 20*, 1−61.
37. Kerr, S. G., and Anderson, K. S. (1997) *Biochemistry 36*, 14056−14063.
38. Patel, P. H., and Preston, B. D. (1994) *Proc. Natl. Acad. Sci. U.S.A 91*, 549−553.
39. Thrall, S. H., Krebs, R., Wohrl, B. M., Cellai, L., Goody, R. S., and Restle, T. (1998) *Biochemistry 37*, 13349−13358.
40. Boucher, C. A., Cammack, N., Schipper, P., Schuurman, R., Rouse, P., Wainberg, M. A., and Cameron, J. M. (1993) *Antimicrob. Agents Chemother. 37*, 2231−2234.
41. Gao, Q., Gu, Z.-X., Parniak, M. A., Cameron, J., Cammack, N., Boucher, C., and Wainberg, M. A. (1993) *Antimicrob. Agents Chemother. 37*, 1390−1392.
42. Tisdale, M., Kemp, S. D., Parry, N. R., and Larder, B. A. (1993) *Proc. Natl. Acad. Sci. U.S.A. 90*, 5653−5656.
43. Doolittle, R. F., Feng, D.-F., Johnson, M. S., and McClure, M. A. (1989) *Q. Rev. Biol. 64*, 1−30.
44. McClure, M. A. (1993) in *Reverse Transcriptase* (Skalka, A. M., and Goff, S. P., Eds.) pp 425−444, Cold Spring Harbor Laboratory Press, Cold Spring Harbor, NY.
45. Harris, D., Yadav, P. N. S., and Pandey, V. N. (1998) *Biochemistry 37*, 9630−9640.
46. Larder, B. A., Kemp, S. D., and Purifoy, D. J. M. (1989) *Proc. Natl. Acad. Sci. U.S.A. 86*, 4803−4807.
47. Preston, B. D., and Dougherty, J. P. (1996) *Trends Microbiol. 4*, 16−21.
48. Drosopoulos, W. C., Rezende, L. F., Wainberg, M. A., and Prasad, V. R. (1998) *J. Mol. Med. 76*, 604−612.
49. Bebenek, K., Abbotts, J., Roberts, J. D., Wilson, S. H., and Kunkel, T. A. (1989) *J. Biol. Chem. 264*, 16948−16956.
50. Hamburgh, M. E., Drosopoulos, W. C., and Prasad, V. R. (1998) *Nucleic Acids Res. 26*, 4389−4394.
51. Wainberg, M. A., Salomon, H., Gu, Z., Montaner, J. S. G., Cooley, T. P., McCaffrey, R., Ruedy, J., Hirst, H. M., Cammack, N., Cameron, J., and Nicholson, W. (1995) *AIDS 9*, 351−357.
52. Nijhuis, M., Schuurman, R., de Jong, D., van Leeuwen, R., Lange, J., Danner, S., Keulen, W., de Groot, T., and Boucher, C. A. B. (1997) *J. Infect. Dis. 176*, 398−405.
53. Skoog, D. A. (1985) in *Principles of Instrumental Analysis*, 3rd ed., pp 7−18, Saunders College Publishing, New York.

BI990709M